

# Finishing and Strengthening of Internal Cylindrical Surfaces by Vibratory-Rolling

BADEA LEPADATESCU  
Department of Manufacturing Engineering  
Transylvania University of Brasov  
B-dul Eroilor nr.29, Brasov  
ROMANIA  
lepadatescu@unitbv.ro

*Abstract:* - The paper presents constructive solutions that enlarge the application domain on the industrial scale of the finishing and hardening process by vibro-rolling. The solution shows the construction of a vibratory head driven by a hydraulic impulse generator. Given the importance of the kinematics of the surface finishing process by vibro-rolling, the paper analytically establishes the link between the kinematic and constructive parameters of the technological system used.

*Key-Words:* - vibro- rolling process, surface finish, work-hardening.

## 1 Introduction

Finishing of surfaces by cold plastic deformation is noticeable by substantial advantages over cutting operations. Obtaining a favorable fiber, making the work-hardening and compressive stresses in the boundary layer, the possibility of obtaining a superior surface finish by improving the initial roughness represents the main advantages and particularities of this process.

Simultaneously with the hardening of the boundary layer by 30-50% compared to the core hardness of the workpiece, a substantial increase of up to 80% of the bearing area ratio capacity of the surfaces thus processed is achieved [1]. As shown in the previous research [3], [4], the deformation action by rolling is even greater as the movements of the deforming element are more complex with respect to the initial surface to be processed.

For this purpose, the classic methods of finishing and work hardening of the metal parts by rolling have been completed with the vibration of the tool or of the rolling element.

The attempts so far [3], [4], intended for the processing of exterior cylindrical surfaces, subsequently extended to the interior cylindrical surfaces, appear to be insufficient to meet the growing productivity requirements of the producers and beneficiaries.

In this regard, the present paper presents some constructive solutions that enlarge the perspective of industrial scale application of the new process.

When solving the problem, were taking into account the purpose of machining - finishing and work hardening – and also the dimensions, the constructive shape and the rigidity of the workpieces intended for processing by this process under the conditions of an increased economic efficiency.

The experimental installation (Fig. 1) was designed for the purpose of machining the internal surfaces of tubes, sleeves of relatively thin wall. This installation consists of an oscillating roller head 2, integral with the vibrator 3, which is connected to a pulse generator.

The impulse generator assembly was mounted on a universal lathe carriage, the clamping and drives device in the mandrel, and the rolling head and the vibrator in the tailstock.

The vibration device is driven by the fluid received from the rotary distributor 5 which is driven by the motor 6 fed to a 24 V and 60 A direct current source. The speed variation is achieved by the rheostat R. The rotary distributor is connected to the hydraulic accumulator 7, fed by a constant flow pump  $Q = 40 \text{ l / min}$  and a pressure  $p_{ef} = 65 \text{ atm}$ . This in turn is acted by the alternating-current motor 11, with  $n = 1461 \text{ rpm}$  and  $P = 4 \text{ kW}$ . The second connection is made to the tank 9. The pressure is controlled by means of the overpressure valve 10. The whole pulse generator assembly is formed by a closed loop hydraulic system.

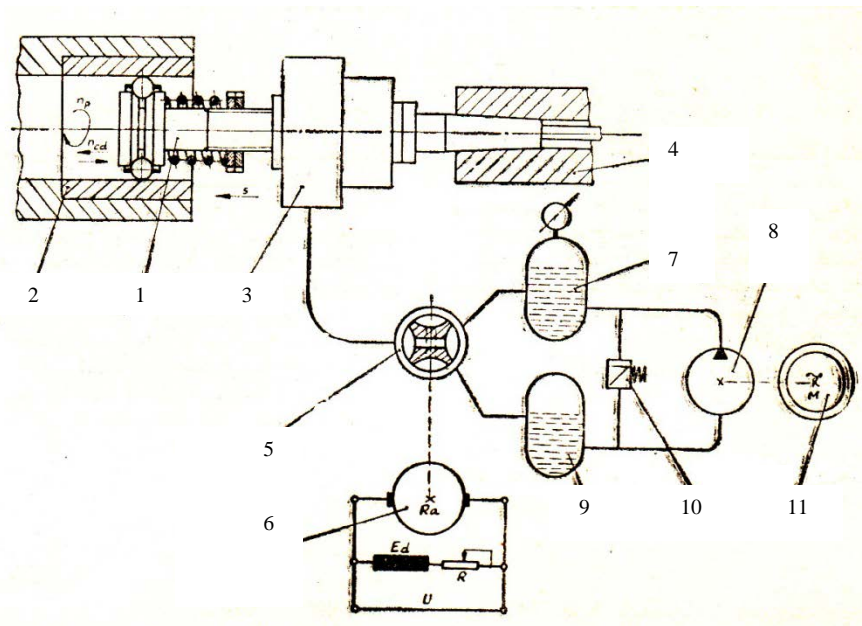


Fig.1 Experimental installation for machining by vibro-rolling.

## 2 Construction of used tools

The choice of a rational tool construction is determined by a large number of factors: the size and shape of the workpieces, their strength and stiffness, the dimensional-geometric accuracy, the character of the production and others.

For the study and experimentation, was adopted the construction of two rolling heads with balls equipped with two cones. One of the rolling heads has the cones and housing of movable balls fixed (Fig.2), and the other has the fixed housing and the cones movable (Fig.3).

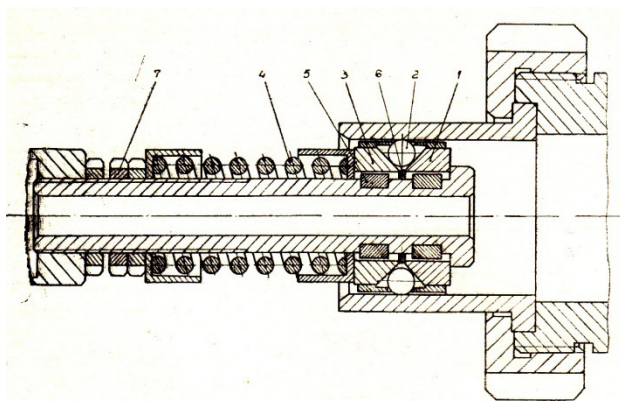


Fig.2 Fixed cone rolling head.

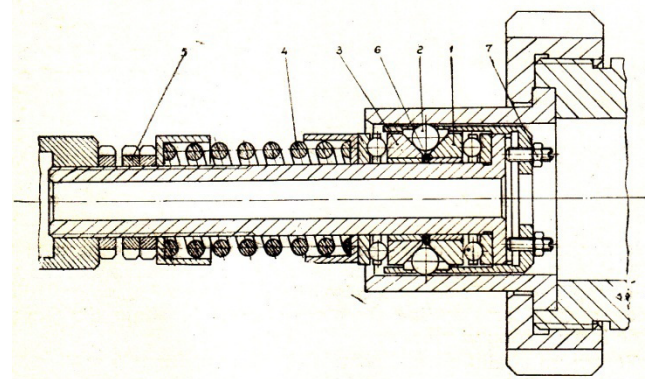


Fig.3 Roller head with mobile cones.

In order to eliminate the danger of producing a metal layer with uneven roughness and tensions, the rolling elements are elastically operated. This elasticity is ensured by the axial displacement of the intermediate cone 3, which transmit to the working balls 2 a maximum operating pressure over the entire circumference of the rolling path, given by a helical spring 4.

Having the aim to avoid the phenomenon of polygonization of the working balls, the rolling head (Fig. 2) must ensure a gyroscopic movement of the rolling elements. In the constructions so far, it has been ensured that one of the attack cones could rotate freely, due to the presence of an axial ball bearing

between the intermediate cone and the compression helical spring 4.

The new simplified construction eliminates the axial bearing and cancels the free rotation motion by inserting of the locking keys 5. The gyroscopic movement of the working balls in the new construction is achieved by adopting different pressure angles  $\alpha_1 \neq \alpha_2$ , at the attack cones, (Fig. 4). As a result of this, the rolling radius of the balls to the axis II-II ( $r_1$  and  $r_2$ ) as well as those of the cones ( $R_1$  and  $R_2$ ) relative to the axis I-I are different, which creates an additional movement of the ball around the axis III-III.

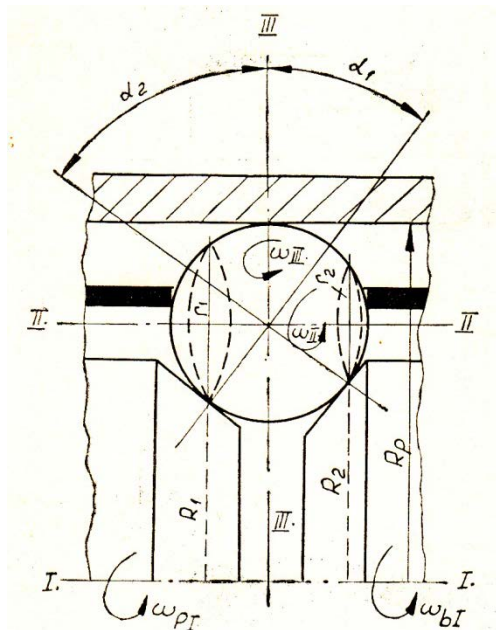


Fig.4 Simplified construction of the rolling head.

### 3 Study of the kinetics of the rolling - vibratory process

In machining by vibro-rolling, the bodies rolling moving in the direction of the feed also performs a vibratory motion in the direction of the axis of the workpiece with certain amplitude.

The trajectory of the ball movement can be approximated by a sinus graph whose amplitude A is

equal to half the length of the vibratory head stroke. For a complete study, the trajectories of two adjacent balls will be analyzed. Their graphical representation on the circumference of the workpiece is shown in Fig.5a, which depicts in a plane, shows as in Fig.5b. The deviation of the balls "x" from the direction of the nominal feed  $S_0$  is characterized by the value:

$$X = A \sin(\omega_s t - \varphi_0) \quad (1)$$

in which: A is the amplitude of the oscillation of the working balls;  $\omega_s$  - the pulsation of the balls, respectively of the rolling head; t - time of origin;  $\varphi_0$  - the initial phase of the rotation of the workpiece or of the rolling head.

As a result of this deviation, the effective feed of the ball " $S_{eb}$ " will be different from its nominal value " $S_{ob}$ ".

The actual feed on the ball, as a measure of the distance between the trajectories of two neighboring balls, measured on the same  $Q_1Q_2$  generators (Fig.6) is given by the relationship:

$$S_{eb} = \Delta_z = Z_1 - Z_2 \quad (2)$$

where:

$$Z_1 = Z_{01} + A \sin(\omega_s t) \quad (3)$$

and

$$Z_2 = Z_{02} + A \sin \left[ \omega_s \left( t - \frac{T_p}{R} \right) \right] \quad (4)$$

in which:  $Z_1$  is coordinate on the  $Q_1Q_2$  generator of the trajectory of the first ball;  $Z_2$  is coordinate to the second balls on the same generator;  $T_p$  is the period of rotation movement of the workpiece; k is the number of rolling bodies (balls).

It can be written as:

$$Z_{01} = \frac{S_{or}}{2\pi} \varphi; \quad Z_{02} = \frac{S_{or}}{2\pi} \left( \varphi - \frac{2\pi}{k} \right)$$

$$T_p = \frac{2\pi}{\omega_p}$$

in which:  $S_{or}$  is the nominal rotation of the tool measured in the axial direction;  $\omega_p$  is the angular speed of the workpiece.

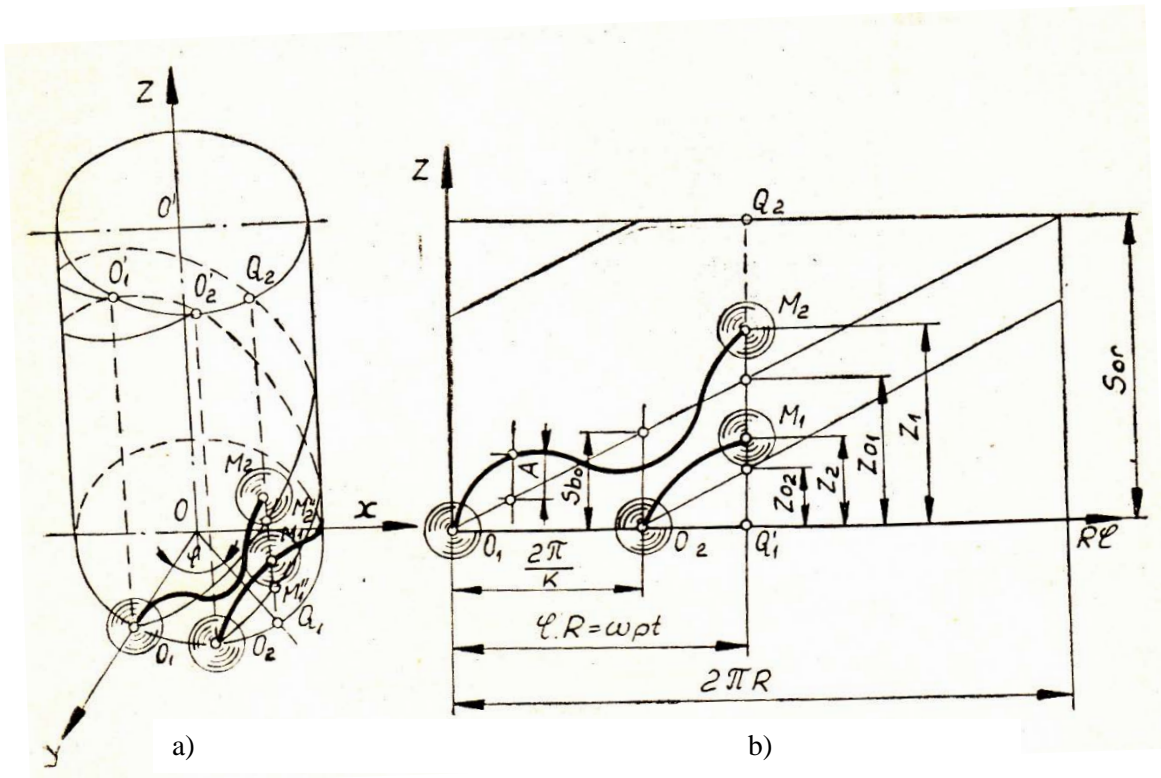


Fig.5 Trajectories of two adjacent balls to the surface of the workpiece.

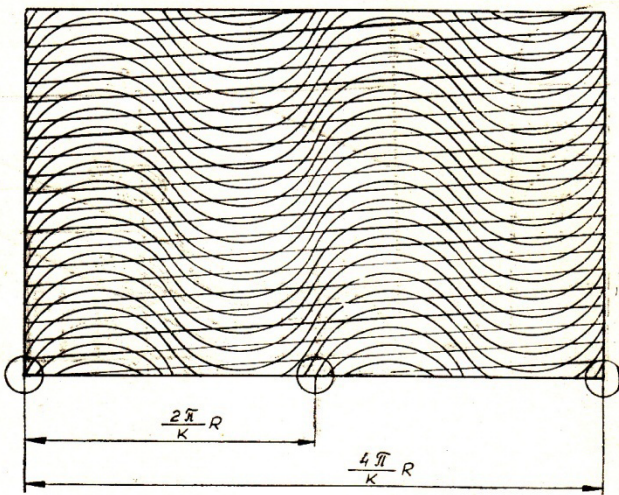


Fig.6 Effective ball trajectory.

After necessary replacements the relationship (2) becomes:

$$\Delta_z = \frac{S_{or}}{k} + A \left[ \sin \omega_s t - \sin \left( \omega_s t - \frac{2\pi \omega_s}{k \omega_p} \right) \right] \quad (5)$$

but:

$$\frac{S_{or}}{k} = S_{ob} \text{ (nominal ball feed)}$$

The sinus difference in relation (5) can be transformed into a product and thus it is obtained:

$$S_{eb} = \Delta_z = S_{ob} + 2A \cos \left( \omega_s t - \frac{\pi \omega_s}{k \omega_p} \right) \quad (6)$$

From the analysis of the relationship (6), the effective feed per ball is given by the sum of the nominal ball feed and the product of the double of the amplitude A with two trigonometric functions of the sinus and cosine, which can take values from -1 to +1 and respectively zero value.

So it can be concluded that for some values of the trigonometric function argument, the actual feed on the ball can remain constant and equal to the nominal value (Fig.6).

For this, it is provided that:

$$f(\omega_s, t, k, \omega_p) = \cos \left( \omega_s t - \frac{\pi \omega_s}{k \omega_p} \right) \sin \frac{\pi \omega_s}{k \omega_p} = 0 \quad (7)$$

Which admits solutions:

$$\text{for: } \sin \frac{\pi \omega_s}{k \omega_p} = 0 \Rightarrow \frac{\omega_s}{\omega_p} = q \cdot k \quad (8)$$

$$\text{and for: } \cos \left( \omega_s t - \frac{\pi \omega_s}{k \omega_p} \right) = 0 \Rightarrow \omega_s =$$

$$(2q + 1) \frac{\pi}{2} \cdot \frac{k \omega_p}{k \omega_p t - \pi} \quad (9)$$

$$q = 1, 2, 3, \dots$$

It is recommended to adopt the solution given by the relation (8) as practically usable by realizing kinematic chains with a rigid link between the two pulses ( $\omega_s$  and  $\omega_p$ ).

To determine the extremes of the function (6) as the case of intersected sinusoidal trajectories (Fig.7), it can also be written as:  $f = \cos(\varphi - \psi) \sin \psi$ , which thus becomes a function of two variables.

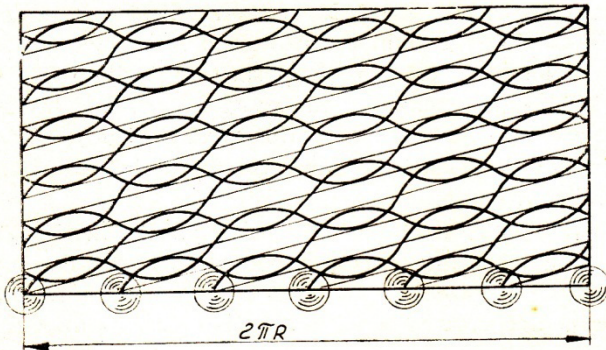


Fig. 7 Intersecting sinusoidal trajectories.

The stationary points of the "f" function are the solutions of the trigonometric system:

$$\begin{cases} \frac{\partial f}{\partial \varphi} = -\sin(\varphi - \psi) \sin \psi = 0 \\ \frac{\partial f}{\partial \psi} = \sin(\varphi - \psi) \sin \psi + \cos(\varphi - \psi) \cos \psi \end{cases}$$

which admit the solutions:

$$\begin{aligned} \psi &= q \cdot \frac{\pi}{2}; \\ \varphi &= (2q^* + 1) \frac{\pi}{2}. \end{aligned}$$

Selecting extremes in the set of static points requires consideration of the discriminant:

$$\Delta = \frac{\partial^2 f}{\partial \varphi^2} \cdot \frac{\partial^2 f}{\partial \psi^2} - \left| \frac{\partial \varphi \partial \psi}{\partial^2 f} \right|^2$$

$$\text{where: } \begin{cases} \frac{\partial^2 f}{\partial \varphi^2} = -\sin \psi \cos(\varphi - \psi) \\ \frac{\partial^2 f}{\partial \varphi \partial \psi} = -\sin(\varphi - 2\psi) \\ \frac{\partial^2 f}{\partial \psi^2} = 2\sin(\varphi - 2\psi) \end{cases}$$

It is known that if:

1.  $\Delta > 0$ , we have as extreme:

for  $\frac{\partial^2 f}{\partial \varphi^2} > 0$  a minimum point,

and for  $\frac{\partial^2 f}{\partial \varphi^2} < 0$  a maximum point.

2.  $\Delta < 0$  we have no extremes.

3.  $\Delta = 0$  the square shape of Taylor's development of the function is semi-defined.

If the values of the second order derivatives in the stationary points  $P(q, q^*) = \left[ q \frac{\pi}{2}, (2q^* + 1) \frac{\pi}{2} \right]$

$$\text{result } \Delta(q, q^*) = \begin{cases} -1 & \text{for even } q \\ 1 & \text{for odd } q \end{cases}$$

The calculation finds that  $f_{max} = 1$  and  $f_{min} = -1$ .

Returning to the initial variables  $\omega_s$ ,  $\omega_p$ ,  $t$  and  $k$ , where  $\omega_s t = \varphi$  and  $\frac{\pi \omega_s}{k \omega_p} \psi$  we result as follows:

$$\omega_s = p \cdot \frac{k}{2} \cdot \omega_p \quad (10)$$

$$\omega_s t = (2q^* + 1) \frac{\pi}{2} \quad (11)$$

In summary, the following conclusions can be drawn:

- If  $q$  is even, we do not have extremes, so the trajectories of the rolling bodies do not intersect;
- If  $q$  is odd, we have extremes, namely, maximum for even  $q^*$  and minimum for odd  $q^*$ .

It is found that when the function has extreme, the trajectories of the sinusoidal shape of the rolling elements intersect forming a network whose density is in function of the ratio  $\omega_s$ ,  $\omega_p$ ,  $A$ , the number of rolling elements  $k$  and obviously the diameter of the workpiece.

In the case of the use of rolling heads of the type shown in Fig.3, the angular velocity of the workpiece  $\omega_p$  with respect to the rolling elements, which behave as fixed markers, can be determined with the relation  $\omega_p = \frac{\pi n_p}{30}$ .

If we use rolling heads of the type shown in Fig. 2, there is a system of moving bodies (workpiece, balls, housing and pressure cones), which can be assimilated cinematically with a planetary mechanism (Fig.8).

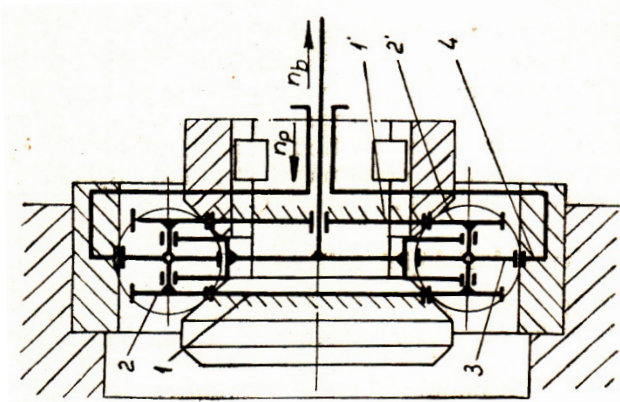


Fig.8 The rolling head assimilated to a planetary mechanism

This time the effective angular velocity of the workpiece  $\omega_e$  is determined by a relation of the form [2]:

$$\omega_{ep} = \omega_{op} \left( 1 - \frac{1}{\left( 1 + \frac{R_1 R_b}{R_2 R_p} \right)} \right)$$

or,

$$\omega_{ep} = \omega_{op} \left[ 1 - \frac{1}{\left( 1 + \frac{1}{\cos \alpha} \right) \left( 1 - \frac{R_b}{R_p} \right)} \right] \quad (12)$$

in which:  $\omega_{op}$  is the nominal angular speed of the blank;  $R_p$  is the inner rolling radius of the blank;  $R_b$  is the radius of the balls;  $R_2$  is the radius of rolling of the balls on the pressure cones;  $R_1$  are the rolling radius of the pressure cones;  $\alpha$  is the pressure angle. From the analysis of the relationship (12) it results that the effective angular velocity  $\omega_{ep}$  is a function of the diameter of the working balls and the pressure angle  $\alpha$ , which is extremely important in determining the ratio between the angular velocity of the workpiece  $\omega_p$  and the pulse of the vibrating head  $\omega_s$ . The type of the network depends of the size of this ratio, which ultimately characterizes the degree of homogeneity of the deformation of the boundary layer and the quality of the surface to be processed.

## 4 Conclusions

Under the conditions shown, the results obtained experimentally showed the possibility of processing the internal cylindrical surfaces at high quality parameters. Thus, when machining a steel workpiece with material OLC 45, with a feed of  $s = 0.12$  mm / rot, rotational speed of the workpiece  $n = 380$  rpm, in the conditions of using a rolling head with six balls ( $k = 6$ ), where a ball-bearing force  $F_b = 30-50$  danN was applied, a surface quality of roughness of  $R_a = 0.2-0.4$   $\mu\text{m}$  was obtained, and an increase in hardness compared to simple rolling of 6-10%.

The research of the vibro-rolling process revealed the following particularities and advantages:

- Vibro-rolling creates the desired microprofile of the surface, with the necessary directions of non-uniformity with the desired number of bearing points per surface unit and the profile that is required to create the optimum conditions for the surface to withstand wear.
- Due to the high vibratory ball deformation capacity and low rolling effort, parts with low stiffness and uneven stiffness can be machined, thus achieving more uniform surfaces in superficial hardness.

### References:

- [1] Blazinski, T. Z., *Plasticity and Modern Metal forming Technology*. New York: Elsevier, 1989.
- [2] Maier, A. – *Work hardening of the superficial layer and finishing the parts through the rolling method*. Experience of company “1 Mai” Ploiesti, ICDT, Bucharest, 1968.
- [3] Hosford, W. F., and R. M. Caddell. *Metal Forming: mechanics and Metallurgy*, 2<sup>nd</sup> ed. Englewood Cliffs, New Jersey: Prentice\_Hall, 1993.
- [4] Lange, K., *Handbook of Metal Forming*. New York: McGraw-Hill, 1985.
- [5] Underwood, L. R., *The Rolling of Metals*, Vol.1. new York: Wiley, 1990.
- [6] Wusatowski, Z., *Fundamentals of Rolling*. New York: Pergamon, 1989.
- [7] Starling, C.W., *The Theory and Practice of Flat Rolling*. London: The University of London Press, 1992.